J Polym Environ (2018) 26:342–354
DOI 10.1007/s10924-017-0950-4

ORIGINAL PAPER

Contribution of Catalytic Transesterification Reactions to the Compatibilization of Poly(lactic acid)/Polycarbonate Blends: Thermal, Morphological and Viscoelastic Characterization

Nadjat Chelghoum[1] · Melia Guessoum[1] · Magali Fois[2] · Nacerddine Haddaoui[1]

Published online: 7 February 2017

Abstract Samarium acetylacetonate (Sm-Acac) was added to catalyze interchange reactions between poly(lactic acid) (PLA) and polycarbonate (PC) in order to promote compatibilization and enhance the performances of the PLA/PC blend. The effects of the composition and catalyzed transesterification reactions were investigated using differential scanning calorimetry (DSC), thermogravimetry (TG), dynamic mechanical thermal analysis (DMTA) and scanning electron microscopy (SEM). DMTA and DSC analysis revealed the immiscibility of the uncatalyzed PLA/PC blends for the studied compositions because the glass transition temperatures of PC and PLA were unchanged after blending. In the PLA glassy region, PLA/PC blends exhibited lower storage moduli which increased upon heating due to the cold crystallization process. During melt mixing with Sm-Acac catalyst, PLA/PC blends were submitted to two competing processes. In one hand, Sm-Acac acted as a plasticizer and contributed in decreasing significantly the glass transition, crystallization and melting temperatures of PLA phase. In the other hand, Sm-Acac proved its efficiency in catalyzing the transesterification reactions that were evidenced by the decrease of the PLA aptitude to crystallization due to the hindering effect of the PC units inserted into the PLA chains. PLA/PC blends melt mixed with 0.25% of Sm-Acac showed a significant strengthening effect, corresponding to an increase in the storage modulus in the temperature range comprised between 70 and 90 °C. This indicated the formation of a copolymer at the interface and the promotion of adhesion as it is confirmed from the decrease in the height of the PLA Tan δ peak. At 0.5% of Sm-Acac, (90/10) PLA/PC blend revealed a new peak assigned to the glass transition of the PLA-PC copolymer, whereas the (50/50) PLA/PC blend was converted into a new random copolymer. TG analysis proved the presence of a copolymer structure presenting an intermediate thermal stability in both the catalyzed and uncatalyzed blends.

Keywords Transesterification · Compatibilization · Poly(lactic acid) · Polycarbonate · Samarium acetylacetonate

✉ Melia Guessoum
guessoum_melia@yahoo.fr

[1] Laboratoire de Physico-Chimie des Hauts Polymères (LPCHP), Département de Génie des Procédés, Faculté de Technologie, Université Ferhat ABBAS Sétif1, Sétif, Algeria

[2] Centre d'Etudes et de Recherche en Thermique, Environnement et Système (CERTES EA-3481), Université Paris Est Créteil, Créteil, France

Introduction

The high brittleness and poor thermal and gas and water vapor barrier properties of PLA are the major obstacles for its diffusion in many conventional and technical fields, such as high temperature applications and packaging [1, 11]. Thus, a lot of attempts have been devoted to promote PLA performances by blending with other polymers and/or incorporating nanoclays and non-biodegradable and biodegradable fillers [12]. In this context, PLA has been melt blended with many polymers, such as polyethylene terephthalate (PET) [13, 14], polyamide (PA) [15], polystyrene (PS) [16], biopolyethylene [17], poly(butylene adipate-co-terephthalate) (PBAT) [18], poly (vinylphenol) [19], thermoplastic starch (TPS) [20], polybutylene succinate (PBS) [21], polyhydroxybutyrate-valerate (PHBV) [22], and polycarbonate (PC) [23]. Nanoclays have been added to PLA to reinforce particularly mechanical properties [2, 24–27], fire retardancy [28], thermal properties [11, 29],

optical properties [30] and barrier performances [31, 32]. Also, PLA bio-composites have been prepared using wood flour [33], lignin [34, 35], cellulose nanocrystals [6, 8, 9, 36, 37] and olive pit [38]. Furthermore, PLA nanocomposites based on metallic nanoparticles, such as zinc oxide (ZnO) [39] and silver (Ag) [9] as antimicrobial agents and titanium dioxide (TiO_2) to promote photodegradability [40] have been investigated. Even these advancements in PLA research, there is still many drawbacks that continue to limit its employment in some sectors which require particular mechanical and thermal properties. Among PLA above cited blends, its combination with PC presenting a high inherent thermal stability and an important tensile strength and elongation at break appears the more attractive strategy to overcome PLA brittleness and poor thermal resistance.

Recently, several studies on PLA and PC blends have been performed to get an idea on the improvements that can be induced by such a combination and on the factors that could influence its performances [41–43]. To improve affinity between the two immiscible components, Lee et al. [41] studied the compatibilizing effect of poly(styrene-g-acrylonitrile)-maleic anhydride (SAN-g-MAH), poly(ethylene-co-octene) rubber-maleic anhydride (EOR-MAH) and poly(ethylene-co-glycidyl methacrylate) (EGMA) on the mechanical, morphological and rheological properties of a (30/70) PLA/PC blend. They concluded that the higher mechanical strength equivalent to the lowest PLA droplet size is obtained at 5 phr (parts per hundred resin) of SAN-g-MAH. On the other hand, Phuong et al. [42] tried the reactive compatibilization of PLA/PC blends via interchange reactions using tetrabutylammonium tetraphenylborate (TBATPB) and triacetin (TA) as a catalytic system. The addition of both TA and TBATPB resulted in improved compatibility through the formation of a PLA-PC copolymer which has a glass transition temperature (T_g) situated between those of PLA and PC, as obtained by dynamic mechanical thermal analysis. As the catalyst was added, the Young's modulus of the materials increased as a result of both the improvement of compatibility and chain scission in the PLA phase, enabling the achievement of co-continuous phase morphology for lower PC contents. Liu et al. [43] investigated the effect of catalysts on the transesterification mechanism between PLA and PC under flow field. They noticed that without catalyst, most of copolymers have relatively high molecular weight with low PC content, which implies that transesterification reaction most likely happens only once between PLA and PC chains during the mixing process, and only a small amount of multiple reactions happen. To promote the transesterification reaction between the two polyesters to a greater extent, three catalysts (zinc borate, titanium pigment and tetrabutyltitanate) have been used. ^1H nuclear magnetic resonance spectroscopy, gel permeation chromatography and dynamic mechanical analysis revealed that catalysts induce more multiple reactions accompanying with the reducing molecular weight in copolymers and increasing PC content. Moreover, it was found that the catalysts, especially tetrabutyltitanate, affect not only the chain compositions of the copolymers, but influence also the amount of polymers involved in the reaction.

In previous papers, Guessoum et al. [44–46] reported the effects of transesterification reactions in presence of tetrabutylorthotitanate (TBOT) on the properties of PC/PET blends. They pointed out the effectiveness of ester-carbonate interchange in the reactive compatibilization of the system. Indeed, they observed that after transesterification reactions, important variations were noticed on the T_g values of both PET and PC, on PET crystallinity, thermal stability and mechanical and rheological properties of the blend. The evaluation of PC and PET weight fractions in PC and PET rich-phases according to Wood and Fox-Couchman equations revealed PC and PET chains segments transfer from a phase to another when the interchange catalyst is added. Several authors [47–53] studied a series of interchange catalysts and found that TBOT was the most efficient but it promotes also secondary reactions. They proved also the efficiency of lanthanide series catalysts such as samarium acetylacetonate in interchange catalyzing but contrary to the later catalyst, it offers the opportunity to control the structure of the system.

In this study, PLA/PC compatibilized blends were prepared via reactive blending in the molten state in presence of samarium acetylacetonate used as a catalyst. The blending conditions such as temperature and time were selected to permit the occurrence of interchange reactions between polymers. The characterization of the catalyzed and uncatalyzed blends focused essentially on the structural, rheological, morphological and thermal properties as a function of the composition.

Experimental

Materials

PLA is a PLI 005 resin manufactured by NaturePlast. It is derived from vegetal resources and has the following characteristics: (melt flow index (MFI) at 190 °C and under 2.16 kg: 10–30 g/10 min, melting temperature: 155–160 °C, degradation temperature: 240–250 °C). PC is supplied by Bayer under the trade name of Makrolon 2858 (MFI at 190 °C: 10 g/10 min, density 1.20 g cm^{-3}). The interchange catalyst is samarium (III) acetylacetonate hydrate ($Sm(acac)_3$) (noted Sm-Acac) which chemical structure is $(C_5H_8O_2)_3Sm.x\ H_2O$purchased from Sigma-Aldrich.

Processing

Before melt mixing, PC, PLA and Sm-Acac were dried in an oven at 60 °C for 24 h. PLA and PC dried granules were manually mixed in different ratios then melt blended in a 60 cm^3 Brabender mixer chamber to get uncatalyzed (90/10), (70/30) and (50/50) (Vol.%) PLA/PC blends. Mixing was conducted at a temperature of 220 °C, a speed of 30 rpm during a mixing time of 15 min. Moreover, PLA/PC catalyzed blends were prepared by incorporating 0.25 and 0.5% of Sm-Acac added directly during blending after the melting of the polymers. Sm-Acac was also added to pure PLA and pure PC in order to investigate its effect on the homopolymers. Torque measurements were carried out during the blending.

Characterization Techniques

Differential Scanning Calorimetry (DSC)

DSC measurements were carried out to investigate the thermal behavior of the materials with a Perkin-Elmer instrument under inert atmosphere. The analysis was performed on approximately a mass of 10 mg according to a three steps program: first heating from 25 to 250 °C at 10 °C/min, cooling from 250 to 25 °C at 10 °C/min, and second heating from 25 to 250 °C at 10 °C/min. Two minutes isothermal plateau was inserted between the ramps. The thermal properties, ie the calorific capacity difference (ΔC_p), the T_g, the crystallization temperature and enthalpy, respectively T_c and ΔH_c and the melting temperature and enthalpy, respectively T_m and ΔH_m were determined from the second heating curves.

Dynamic Mechanical Thermal Analysis (DMTA)

Specimens of the neat homopolymers and catalyzed and uncatalyzed blends of dimensions (50 × 10 × 1) mm^3 were subjected to the dynamic mechanical analysis using a Discovery HR-2 from TA instrument. The measurements were carried out in shearing mode and corresponding viscoelastic properties were determined as a function of temperature. The temperature range used in the present investigation was varied from 25 to 180 °C with a heating rate of 3 °C min^{-1} The samples were scanned at a fixed frequency of 1 Hz with a dynamic strain of 0.05%.

Thermogravimetric Analysis (TGA)

Thermogravimetric analysis was performed using a Perkin Elmer TGA 4000. Measurements were carried out by heating the samples from 25 to 700 °C at a heating rate of 10 °C min^{-1} under a flow of nitrogen gas.

Scanning Electron Microscopy (SEM)

The morphology of the catalyzed and uncatalyzed blends was studied by scanning electron microscopy using a JSM-6301F microscope. The analysis was performed by the observation of the surfaces produced on fracturing at liquid nitrogen temperature and after coating with a conductive layer of gold.

Solubility Measurements

This test was carried out by placing a sample of 100 mg (m_0) of neat, 0.25 and 0.5% Sm-Acac catalyzed (50/50) PLA/PC blends in a volume of 30 ml of cyclohexanone heated at 30 °C. After stirring for a period of 24 h at 300 rpm, the suspension was filtered and the insoluble fraction was recovered, dried then weighted (m). The solubility was evaluated according to the following equation:

$$\text{Solubility } (\%) = \left(\frac{m_0 - m}{m_0}\right) \times 100$$

Results and Discussion

Thermal Characterization of PLA and PC Homopolymers

The DSC thermograms of PLA and PC homopolymers before and after compounding with Sm-Acac catalyst are presented in Fig. 1. During the first heat, a peak associated with physical ageing is superimposed with the PLA glass transition. This peak disappears at the second heat allowing measuring the T_g of PLA at 59.2 °C. The cold

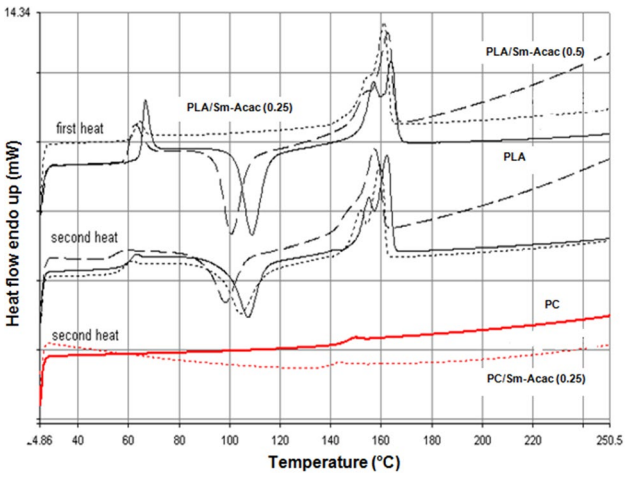

Fig. 1 DSC thermograms of PLA and PC homopolymers compounded with and without Sm-Acac catalyst

crystallization peak appears between 80 and 135 °C with a crystallization temperature taken at the onset of 99 °C. The melting of pure PLA shows a double peak that presents two melting temperatures T_{m1} and T_{m2} close to 150.5 and 156 °C, respectively, indicating the presence of two types of crystalline populations with different degrees of perfection. In this context, several studies reported that the crystalline phase of PLA depends on the processing temperature for crystallization [42, 54]. The pseudo-orthorhombic disordered α' and orthorhombic ordered α PLA's crystalline phases are formed at crystallization temperatures lower than 100 °C and higher than 120 °C, respectively [55]. The small difference between the cold crystallization and melting enthalpies indicates that PLA presents a low crystallinity at ambient temperature. The calculation of the PLA crystallinity using the crystallization peak during cooling and an enthalpy of a pure crystal ΔH_m° of 93 J/g [55] gives an approximate value of 3%. PC thermogram exhibits a glass transition temperature at about 145 °C (ΔC_p=0.21 J g^{-1} $°C^{-1}$).

After compounding with weight fractions of 0.25 and 0.5% of Sm-Acac catalyst, PLA T_g shifts from 59.2 to 56.6 and 54.6 °C, respectively. At the same time, the cold crystallization and the melting temperatures decrease. Also, the melting behavior of the PLA melt mixed with 0.5% of Sm-Acac reveals a double peak where the low temperature disordered α' phase amplitude decreases in favor of the ordered α phase due to the improved chains mobility. PC homopolymer shows the same trend; its T_g decreases from 145 to 139 °C after compounding with 0.25% of Sm-Acac. The decrease in the T_gs of both polymers proves that Sm-Acac catalyst acts also as a plasticizer.

To investigate the effects of Sm-Acac, time dependent curves of torque for PLA, PC and (50/50) PLA/PC blends prepared with 0.25 and 0.5% of Sm-Acac are studied. Usually, torque variations versus time show in the beginning, an increase resulting from the resistance of the polymer that has not yet reached the melt. Thereafter, the torque decreases when the polymer attains the melt and all the interchain interactions have been destructed. Finally, it reaches a constant value as a plateau which expresses the torque at stability.

Figure 2 depicts the torque evolution for PLA, PC and (50/50) PLA/PC blends. PC presents the higher torque at stability which is evaluated at approximately 30 N m. In opposite, PLA depicts lower torque values and shows at stability a torque of about 1.07 N m (50/50) uncatalyzed PLA/PC blend presents intermediate torque values between those of PC and PLA. During melt mixing with 0.25% of Sm-Acac, lower torque values are recorded relatively to the uncatalyzed blend, due to the contribution of Sm-Acac plasticizing effect in reducing the mixture viscosity. A more important decrease of the mixing torque is observed after increasing the catalyst concentration to 0.5%. The contribution of the PC phase which should provide a higher viscosity to the blend is no longer observed and the blend's torque approaches the PLA one after 9 min of mixing due to the occurring of important structural changes.

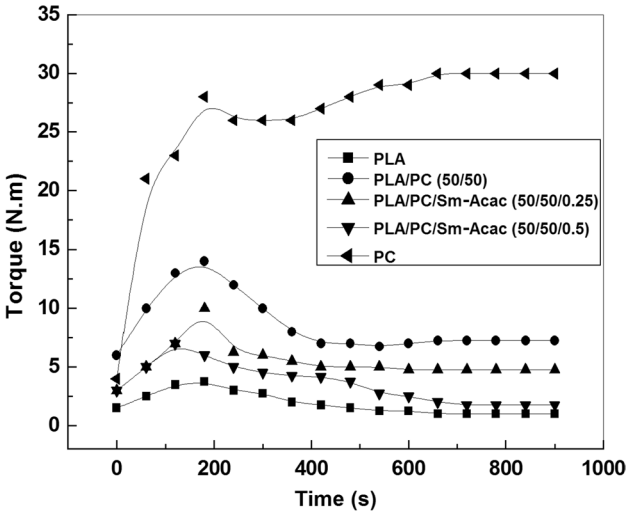

Fig. 2 Time dependent curves of torque for PLA, PC and (50/50) PLA/PC blends

Viscoelastic Characterization of Uncatalyzed and Catalyzed PLA/PC Blends

Figure 3a, b depict, respectively, the variations of the storage modulus G' and the damping factor (Tan δ) as a function of temperature for PLA, PC and PLA/PC uncatalyzed blends. In the glassy region, PLA presents a storage modulus of about 1141 MPa. The drop of the storage modulus observed around 63 °C is attributed to the glass transition and corresponds also to a peak in the variations of Tan δ (Fig. 3b). Afterwards, an increase in the modulus is observed due to the cold crystallization process. This behavior is attributed to an increase in the PLA stiffness caused by the ability of the amorphous regions to reorganize into crystallites upon heating [56–58]. At ambient temperature, PC presents a storage modulus of about 544 MPa which drops around 145 °C indicating the PC glass transition. This corresponds to a peak visible on the Tan δvariations which exhibits a maximum around 151 °C.

At ambient temperature, the storage moduli of PLA/PC blends are intermediate between those of the homopolymers. After a first drop around the PLA glass transition, storage moduli increase again due to PLA cold crystallization and form a plateau which persists until the second drop corresponding to the PC glass transition is attained. The T_gs of the PLA and PC phases are unchanged proving the immiscibility of the blends. As the PLA content decreases,

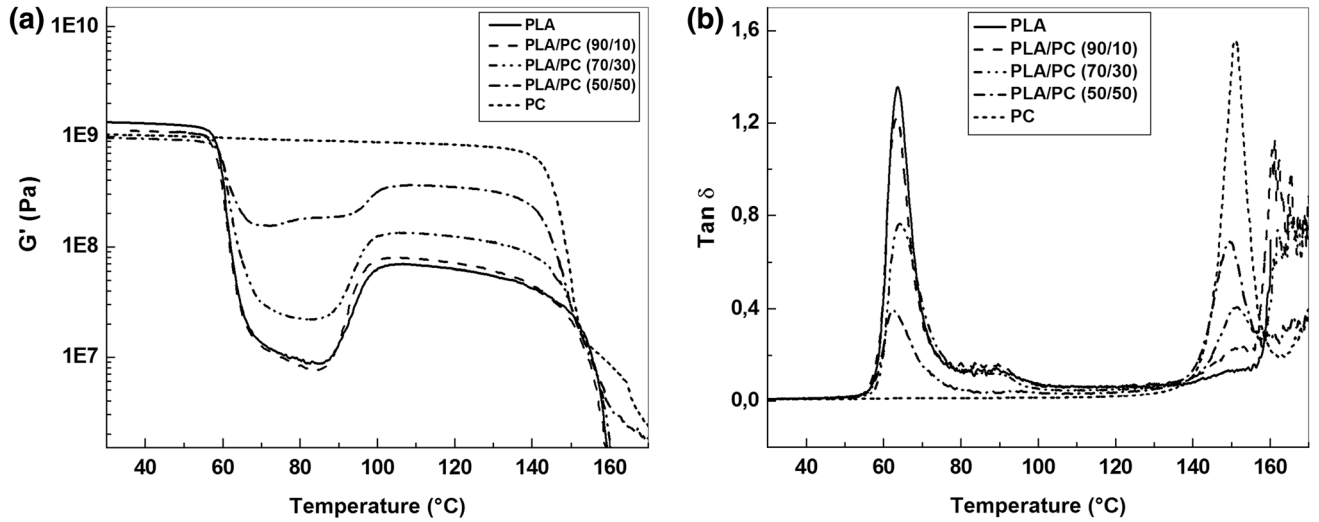

Fig. 3 DMTA thermograms of PLA, PC and uncatalyzed PLA/PC blends: **a** storage modulus and **b** Tan δ

the drop of the blends storage modulus around the PLA glassy region decreases. Moreover, in the temperature zone where the PLA cold crystallization occurs, the crystallization temperature and the storage modulus increase with increasing the PC content into the blends. A slight enhancement in the storage modulus of the (50/50) PLA/PC blend is observed in this temperature range and could result from the establishment of strong interactions between the PLA and PC phases. This indicate the occurring of exchange reactions like it was found by Liu et al. [43] who suggested that transesterification occurs but in a lower extent when PLA and PC are melt blended without catalyst. The height of the Tan δ peak depends on the molecular mobility of the amorphous regions in the polymer [59] and the Tan δ area is related to the content of amorphous phase [60]. As the PC concentration increases, the height of PLA Tan δ peak decreases, while the PC peak becomes higher.

Figure 4a, b represent, respectively, the variations of the storage modulus and Tan δ as a function of temperature for the PLA/PC blends catalyzed with 0.25% of Sm-Acac. T_g of PLA decreases for all the compositions due to the Sm-Acac plasticizing effect. An identical result was reported by Phuong et al. [42] on using triacetin as a catalyst. In the temperature range where the PLA cold crystallization begins, the storage modulus of the catalyzed blends does not decrease as it occurs for the (90/10) and (70/30) uncatalyzed systems, but it increases notably as the PC content increases. The reinforcing effect is situated in the same

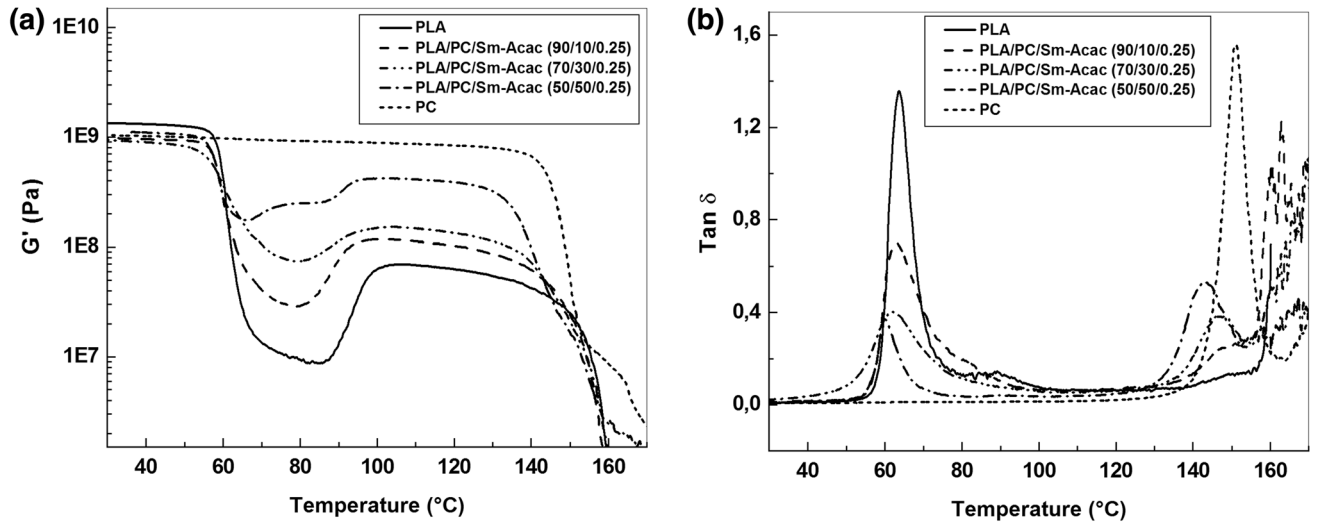

Fig. 4 DMTA thermograms of PLA/PC blends prepared with 0.25% of Sm-Acac catalyst. **a** Storage modulus and **b** Tan δ

temperature range as for the uncatalyzed (50/50) PLA/PC blend, but it is more intense and concerns all the compositions. The observed strengthening suggests an enhancement of the blends stiffness even though the Sm-Acac catalyst plasticization. This behavior seems to be due to the promotion of adhesion and the reinforcement of the interface after the occurring of interchange reactions resulting in the generation of a copolymer phase. In this context, it has been proposed that the transesterification mechanism of PLA and PC is mainly direct ester–ester interchange reaction. The occurrence of the exchanges between the PLA and PC segments is favored by the proximity of the ester groups and their high density in the interface. Also, the PLA chains need to have sufficient contact time with the PC ones as compared to the reaction time. The role of the catalyst is to speed up the reaction and to increase the average reaction time to form copolymers [43]. The exchange reaction leads initially to the formation of block copolyesters, and with the reactive proceeding, random copolyesters progressively are formed [46]. Furthermore, the decrease in the height of PLA Tan δ peak observed in Fig. 4b (by comparison with Fig. 3b) may be interpreted as being due to the creation of chemical links between PLA and PC phases. Indeed, for composite materials, the intensity of Tan δ peak is inversely proportional to the interfacial resistance [61, 62]. Chemical links created between PLA and PC phases may also result in the diminution of the PLA chains mobility inducing a limited crystallization of PLA. Also, the storage modulus plateau narrows because the PLA crystallization temperature increases and the PC phase T_g decreases when the PC content into the blends increases.

Figure 5a, b depict, respectively, the variations of the storage modulus and Tan δ as a function of temperature for PLA/PC blend catalyzed with 0.5% of Sm-Acac. For (90/10/0.5) and (70/30/0.5) PLA/PC/Sm-Acac blends, the Sm-Acac plasticization decreases significantly the T_g of the PLA phase and the blends storage modulus around the glassy region, but promotes considerably the PLA cold crystallization due to the enhancement of the chains mobility. This is confirmed by the significant increase observed on the height of the PLA Tan δ peak (Fig. 5b). Additionally, after the PLA glass transition, the Tan δ amplitude of (90/10/0.5) PLA/PC/Sm-Acac blend is increased until 85 °C. This may correspond to the same phenomenon as that observed in pure PLA after its glass transition. An identical peak was observed when studying PET thermal properties and was attributed to the melting of crystals during the PET cold crystallization [63]. Also, the appearance of this peak could be assigned to an additional rigid amorphous phase resulting from the formation of a copolymer phase. Interestingly, the (50/50/0.5) PLA/PC/Sm-Acac blend yields a new material consisting of a PLA-PC random copolymer. This structure is confirmed from the absence of the PLA cold crystallization and the disappearance of the T_gs of PLA and PC phases. The obtained copolymer is based on PLA units linked randomly to PC ones providing a new amorphous material with an intermediate T_g around 72 °C. The PLA-PC copolymer exhibits a higher storage modulus than those observed for PLA and the other PLA/PC blends melt mixed with 0.5% of Sm-Acac. After the glass transition, the storage modulus decreases abruptly. This observation agrees with the results of Liu et al. [43] and Phuong et al. [42] who concluded no changes on the T_gs of PC and PLA phases melt mixed with a catalyst, but they observed a new T_g comprised between those of the two homopolymers that they have assigned to a new PLA-PC copolymer phase.

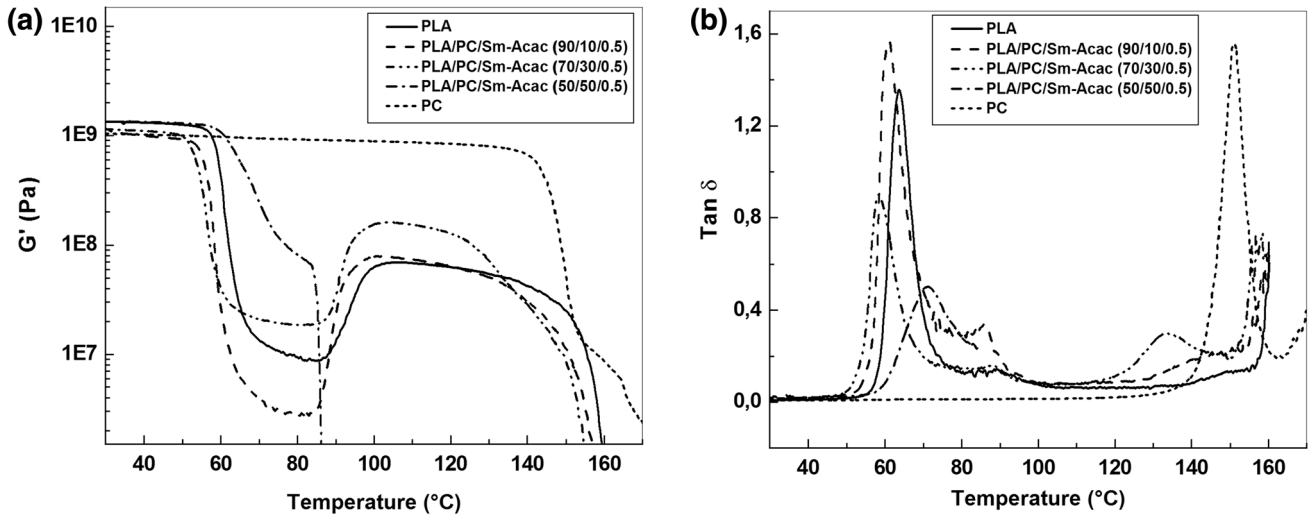

Fig. 5 DMTA thermograms of PLA/PC blends prepared with 0.5% of Sm-Acac catalyst. **a** Storage modulus and **b** Tan δ

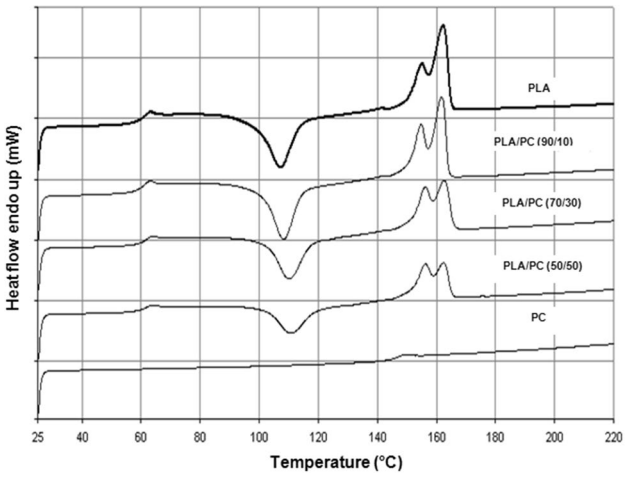

Fig. 6 DSC thermograms of PLA, PC and uncatalyzed PLA/PC blends

Thermal Properties of Uncatalyzed and Catalyzed PLA/PC Blends

Figure 6 shows the DSC thermograms of PLA/PC blends melt mixed without the catalyst. The T_g of the PLA phase is unchanged while that of the PC phase cannot be observed because it is in the temperature range wherein the PLA melting begins. The no shifting of the PLA phase T_g suggests the total immiscibility of the two polymers for all the compositions. The PLA weight fractions(ω) inside the samples were calculated using the ΔC_p values at its glass transition (Table 1). Also, the blends thermograms reveal that the crystallization temperature of PLA shifts to higher values as the PC rate increases. This indicates that PC, which is still in its glassy state, disrupts the reorganization of PLA chains during the crystallization process. Moreover, at the beginning of PLA melting, PC glass transition occurs avoiding the possibility to calculate the PLA melting enthalpy correctly. Nevertheless, it was evaluated considering that the small step introduced by the PC glass transition is trivial compared to peaks (0.2 mW). The crystallinity attained by the PLA into the blends after the cold crystallization was calculated, using the PLA weight fraction, by dividing the melting peak area by the PLA mass (Table 2).

DSC thermograms of PLA/PC blends prepared with 0.25% of Sm-Acac are presented in Fig. 7. As for the homopolymer, the glass transition, crystallization and melting temperatures of PLA inside the (90/10/0.25) and (70/30/0.25) PLA/PC/Sm-Acac blends decrease, confirming the plasticizing effect exerted on the PLA phase. The (50/50/0.25) PLA/PC/Sm-Acac shows also a decrease in the glass transition and melting temperatures because of the Sm-Acac plasticization, but in opposite, it exhibits a higher crystallization temperature relatively to the former compositions. The crystallization peak intensity decreases notably and shifts to higher temperatures because of the lower aptitude of PLA chains to crystallize. At the same time, the two melting peaks move to lower temperatures. The crystallization behavior of the (50/50/0.25)system could be explained by the transfer of PC units into the PLA phase. The resulting copolymer chains present a relatively low tendency to crystallization due to the bulky PC units which hinder their organization into crystals. Significant additional changes confirming the efficiency of Sm-Acac as an active transesterification catalyst are provided by Fig. 8 presenting the thermograms of PLA/PC blends prepared with 0.5% of Sm-Acac. The thermogram of the (90/10/0.5) PLA/PC/

Table 1 DSC thermogram analysis for PLA and uncatalyzed PLA/PC blends

PLA/PC	Glass transition (50–67 °C)			Cold crystallization (80–135 °C)			Melting (135–170 °C)			
	T_g (°C)	ΔC_p (J g^{-1} $°C^{-1}$)	ω(%)	T_c (°C)	Peak area (mJ)	ΔH_c (J g^{-1})	T_{m1} (°C)	T_{m2} (°C)	Peak area (mJ)	ΔH_m (J g^{-1})
100/0	59.2	0.517	100	98.8	334.0	33.4	150.5	156	363.1	36.3
90/10	59.4	0.431	83	100.7	324.4	31.2	150.6	156.5	331.4	31.9
70/30	60.2	0.349	68	102.2	258.6	24.6	151.3	159	267.3	25.5
50/50	60.0	0.262	51	102.0	185.9	17.9	151.2	159.3	201.7	19.4

Table 2 Analysis of DSC thermograms for PLA homopolymer and PLA in PLA/PC blends melt mixed without and with Sm-Acac catalyst

PLA/PC	T_g (°C)			T_c (°C)			T_{m1} (°C)			T_{m2} (°C)		
Sm-Acac	0	0.25	0.5	0	0.25	0.5	0	0.25	0.5	0	0.25	0.5
100/0	59.2	56.6	54.6	98.8	96.7	89.1	150	141	140	156	153	149
90/10	59.4	56.8	54.0	100.7	96.9	90.8	150	146	139	156	154	148
70/30	60.2	55.6	51.4	102.2	96.0	99.5	151	145	130	159	158	136
50/50	60.0	50.3	–	102.0	98.8	–	151	132	–	160	145	–
0/100	145	139	–	–	–	–	–	–	–	–	–	–

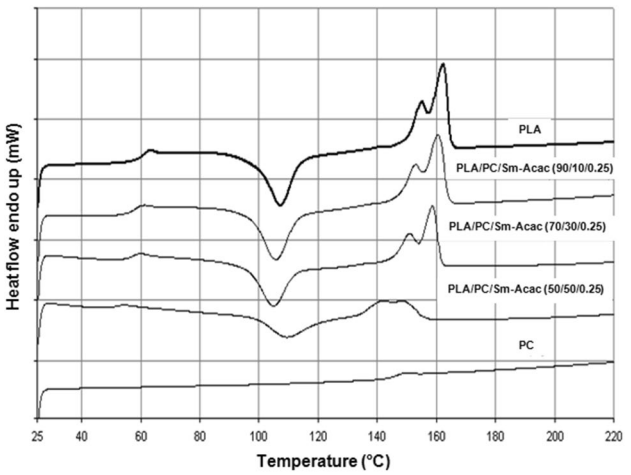

Fig. 7 DSC thermograms of PLA/PC blends prepared with 0.25% of Sm-Acac catalyst

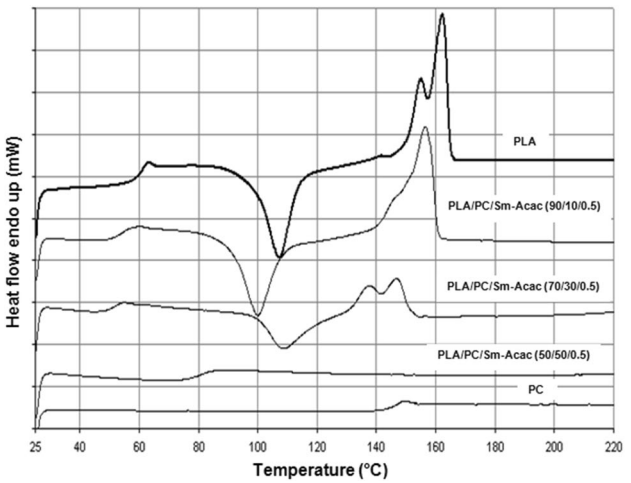

Fig. 8 DSC thermograms of PLA/PC blends prepared with 0.5% of Sm-Acac catalyst

Sm-Acac blend reveals a noticeable decrease in the glass transition, crystallization and melting temperatures of the PLA phase due to the high Sm-Acac plasticization effect. The PLA phase melting behavior is similar to that of the PLA/Sm-Acac system melt mixed with 0.5% of Sm-Acac. The PLA phase into the (70/30/0.5) PLA/PC/Sm-Acac blend shows a lower T_g, but in opposite, the crystallization peak shifts to higher temperatures. This is a contradictory result because, the higher is the Sm-Acac concentration, the greater should be the plasticizing effect and the chains mobility. So, as for the (50/50/0.25) PLA/PC/Sm-Acac, this suggests that copolymer chains resulting from transesterification reactions between PLA and PC are formed. The rigid PC blocks limit strongly the molecular mobility and hinder the PLA crystallization process. Finally, as observed in DMTA analysis, a new random type PLA-PC amorphous copolymer is provided by the (50/50/0.5) PLA/PC/Sm-Acac blend and shows an intermediate T_g value of 80 °C as evaluated from the second heating scan. This finding is extremely important given the interesting properties that this copolymer is expected to present by combining features of both polymers, especially the biodegradability of PLA and the good thermal performances of PC.

In summary, the thermal behavior of PLA/PC/Sm-Acac blends is governed by two antagonist processes resulting from the fact that the Sm-Acac catalyst is not only involved in catalyzing transesterification reactions between PLA and PC, but it acts also as a plasticizer. In one hand, the plasticizing effect of the Sm-Acac catalyst decreases the glass transition temperature of PLA and PC. In the other hand, its action on the cold crystallization process is balanced by the transfer of bulky PC units into the PLA phase which explain the increase in the crystallization temperature for certain compositions. Additionally, it seems that the important decrease in the PC phase T_g does not only result from the Sm-Acac plasticization and the PLA melt, but it may also be due to the insertion of relatively highly mobile PLA units transferred into the PC phase via interchange reactions. A similar result was observed for the PC/PET system, where it was concluded that the shifting to lower temperatures of the PC phase T_g is due to the PET units transfer occurring through TBOT catalyzed transesterification [44].

It is worth noting that the T_g of the random copolymer is comprised into the temperature range where the strengthening effect noticed for the PLA/PC blends catalyzed with 0.25% of Sm-Acac is observed. This supports that, initially, the reinforcement results from a block copolymer localized at the interface. At 0.25% of Sm-Acac, the interchange processes are limited, so the PC and PLA blocks are sufficiently long and exhibit the same T_gs as the corresponding polymers. After increasing the Sm-Acac concentration to 0.5%, inter- and intra-chain transesterification reactions occur and cause the blocks shortening until randomization that produces new copolymer chains with their own T_g.

To get more information on the blends composition and confirm the DSC and DMTA results, the solubility test which gives a rather precise approach of the exchange rate occurring in a system was performed. It is based on the selective solubility of one of the components of a mixture in a solvent and on the change of the behavior of these components with respect to same solvent after the structural changes resulting from transesterification. Consequently, the solubility measurements provide very useful information on the interchange reactions rate and on the structure of the formed copolymer (block or random structure). In this purpose, we used cyclohexanone which dissolves the PC and not the PLA.

The solubility measurement on the uncatalyzed (50/50) PLA/PC system leads to a partial solubility of about 52%. The insoluble fraction contains only the PLA contribution into the sample. However, the blend compounded with 0.25% of Sm-Acac shows a decrease in the solubility to 28%, due to the conversion of the homopolymers at the interface to a block copolymer consisting of long sequences of PLA and PC units and presenting a limited solubility. This result supports the DSC and DMTA findings which attributed the increase in the crystallization temperature of PLA to the copolymer structure formed from the insertion of bulky PC units into the PLA chains via transesterification reactions. Finally, the (50/50) PLA/PC mixture melt mixed with 0.5% Sm-Acac is completely dissolved in cyclohexanone, which suggests that active exchanges between the two polymers occurred. The solubility of this blend was expected, accordingly to the DMTA and DSC results which supports the randomness of the obtained PLA-PC copolymer. Identical results have been obtained by several other authors [46–48].

Thermal Stability of Uncatalyzed and Catalyzed PLA/PC Blends

Thermogravimetric analysis was performed to evaluate the effects of PC concentration and catalytic transesterification reactions on the thermal stability of PLA/PC blends. The degradation parameters, including temperatures at which starts and finishes the decomposition, noticed T_{d0} and $T_{df,}$ respectively, the temperature at maximum weight loss (T_{dmax}) and the decomposition rate (V_d) are evaluated from the thermograms representing the variations of the weight loss (TG) and the derivative of the weight loss versus time (DTG).

Figure 9a, b depict, respectively, TG and DTG thermograms for PLA, PC and uncatalyzed PLA/PC blends. PLA decomposition is carried out in a single step that extends from 295 to 388 °C. The weight loss at T_{dmax} of approximately 358 °C is around 56%, corresponding to a degradation rate of 2.83%/min. The thermal stability of PC is higher because degradation, which occurs also in a single stage, begins around 410 °C, reaches a maximum at 521 °C and ends at 627 °C with a solid residue of 23.61%. The maximum rate of weight loss is about 0.93%/min. Uncatalyzed PLA/PC blends present an intermediate thermal stability. In fact, the thermogram of the (90/10) PLA/PC system shows a decomposition in a single step and reveals a slight increase in the degradation temperatures, whereas the (70/30) and (50/50) blends thermograms exhibit principally two steps corresponding to the decomposition of PLA and PC phases. In these blends, the T_{dmax} of the PLA phase is not affected contrary to that of the PC phase which moves to lower temperatures. This fact has already been observed by Phuong et al. [42], who explained that this could be due to the PLA degradation that would have accelerated the PC phase decomposition. The (50/50) PLA/PC blend exhibits a supplementary small peak in the DTG thermogram that could correspond to the blend's third phase which caused the slight strengthening effect observed in the variations of the storage modulus.

Figure 10a, b represent, respectively, the TG and DTG thermograms of PLA, PC and PLA/PC blends after compounding with 0.25% of Sm-Acac. The Sm-Acac interchange catalyst affects notably the thermal stability of PLA and PC which decomposition parameters slide towards lower temperatures. Also, the thermal stability of PLA/PC/Sm-Acac blends decreases and their decomposition parameters are lower relatively to those of the pure mixtures

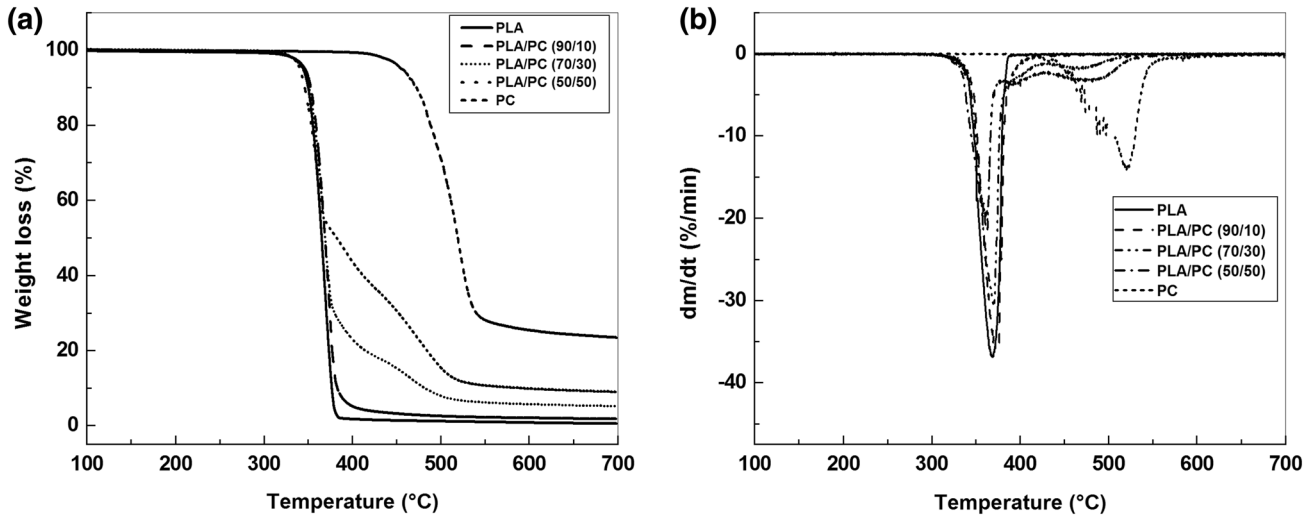

Fig. 9 TG (**a**) and DTG (**b**) thermograms of PLA, PC and uncatalyzed PLA/PC blends

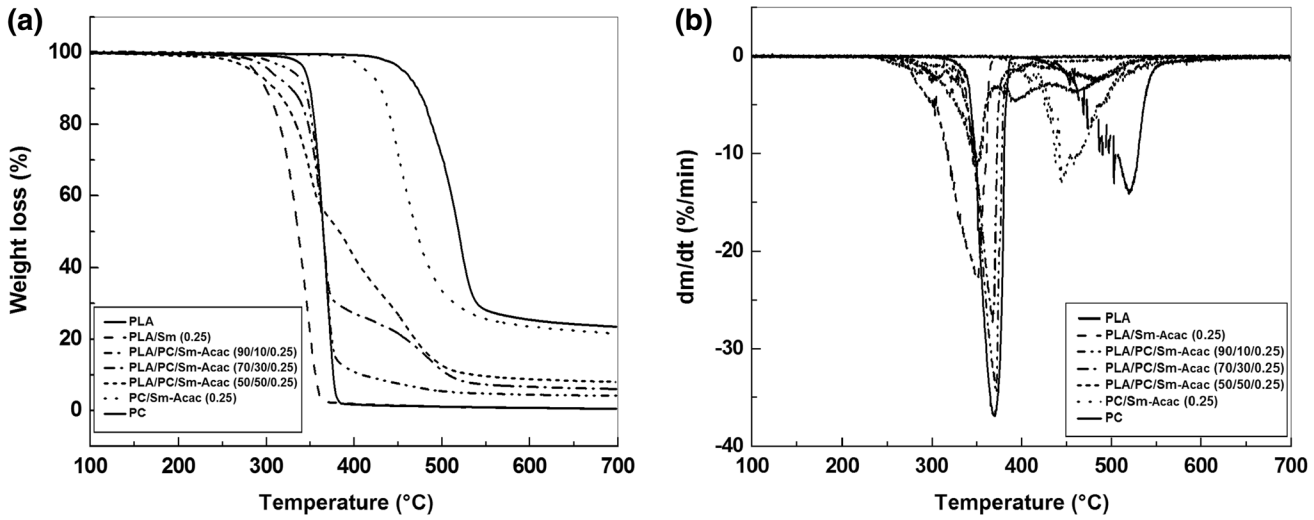

Fig. 10 TG (**a**) and DTG (**b**) thermograms of PLA, PC and PLA/PC blends prepared with 0.25% of Sm-Acac

(Table 3). Nevertheless, the catalyzed blends present a higher thermal stability relatively to the PLA melt mixed with the same concentration of Sm-Acac catalyst due to the contribution of the PC phase. (90/10) reveal decomposition in only one stage while (70/30/0.25) and (50/50/0.25) PLA/PC/Sm-Acac blends decompose in three ones. The first stage of degradation of (70/30/0.25) PLA/PC/Sm-Acac blend begins around 271 °C and finishes at about 317 °C. It corresponds probably to the thermal decomposition of Sm-Acac catalyst [64]. Thereafter, the second and third stages follow and are attributed, respectively, to PLA and PC phases degradation. In addition to these phases decomposition depicted by the first and third stages, respectively, the DTG thermogram of (50/50/0.25) PLA/PC/Sm-Acac blend reveals also an intermediate degradation stage. This additional peak, also observed in the DTG curve for the uncatalyzed (50/50) PLA/PC blend but in a minor intensity, extends from 377 to 432 °C and exhibits a maximum at 395 °C. Its appearance supports the presence into the blend of a copolymer phase presenting a structure different from those of the homopolymers but deriving from them. The intensification of the peak corresponding to this phase suggests that its concentration into the blend increased after blending with the catalyst, which agrees with the DMTA results. The decomposition parameters of PLA, PC and catalyzed and uncatalyzed blends are summarized in Table 3.

Table 3 Decomposition parameters of PLA, PC and uncatalyzed and catalyzed PLA/PC blends

	0% Sm-Acac					0.25% Sm-Acac				
Parameter	100/0	90/10	70/30	50/50	0/100	100/0	90/10	70/30	50/50	0/100
First stage of decomposition										
T_{d0} (°C)	295	302	308	311	410	237	282	271	242	364
T_{df} (°C)	388	417	428	432	627	379	410	317	377	603
T_{dmax} (°C)	368	370	368	362	521	348	370	302	351	446
V_d (%/min)	2.83	2.43	2.17	1.70	0.93	1.72	1.86	1.68	1.64	1.32
Weight loss (%)	1.28	2.13	–	–	23.61	0.88	4.22	–	–	21.8
Second stage of decomposition										
T_{d0} (°C)	–	–	426	346	–	–	–	317	377	–
T_{df} (°C)	–	–	535	422	–	–	–	408	432	–
T_{dmax} (°C)	–	–	470	376	–	–	–	370	395	–
Weight loss (%)	–	–	5.50	17.51	–	–	–	–	–	–
Third stage of decomposition										
T_{d0} (°C)	–	–	–	432	–	–	–	408	432	–
T_{df} (°C)	–	–	–	541	–	–	–	545	555	–
T_{dmax} (°C)	–	–	–	477	–	–	–	483	495	–
Weight loss (%)	–	–	–	9.20	–	–	–	6.43	8.43	–

Morphological Study of PLA/PC Blends

The evolution of the PLA/PC blend morphology with the composition, before and after compatibilization through the addition of the transesterification catalyst is described by the micrographs given by the Fig. 11a–f. Micrographs (a) and (c) showing the morphology of (90/10) and (70/30) PLA/PC blends prepared without Sm-Acac, respectively, exhibit PC droplets dispersed into the PLA matrix. The interface between the domains of the two polymers reveals the existence of voids attributed to the poor adhesion due to their immiscibility. PC droplets present different sizes varying from 13 to 2 µm for the (90/10) PLA/PC blend and from 40 to 2 µm for the composition (70/30). The micrographs (b) and (d) of the same compositions prepared with 0.25% of Sm-Acac show a similar morphology but the PC droplets exhibit smaller dimensions, from 11 to 1.5 µm for the (90/10) PLA/PC blend and from 18 to 1.5 µm for the (70/30) system. The dispersion refinement may result from the contribution of the copolymer to the stabilization of the PC droplets against coalescence. The micrographs (e) and (f) representing the (50/50)PLA/PC system prepared without and with 0.25% Sm-Acac, respectively, reveal a change from the droplet/matrix to the co-continuous morphology resulting from the equivalent rates of the two polymers into the blend. PLA domains show a good adhesion to the PC ones even if they are melt mixed without the Sm-Acac catalyst. The observed morphology agrees perfectly with the DMTA and TG results which mentioned the presence of a third phase at the interface.

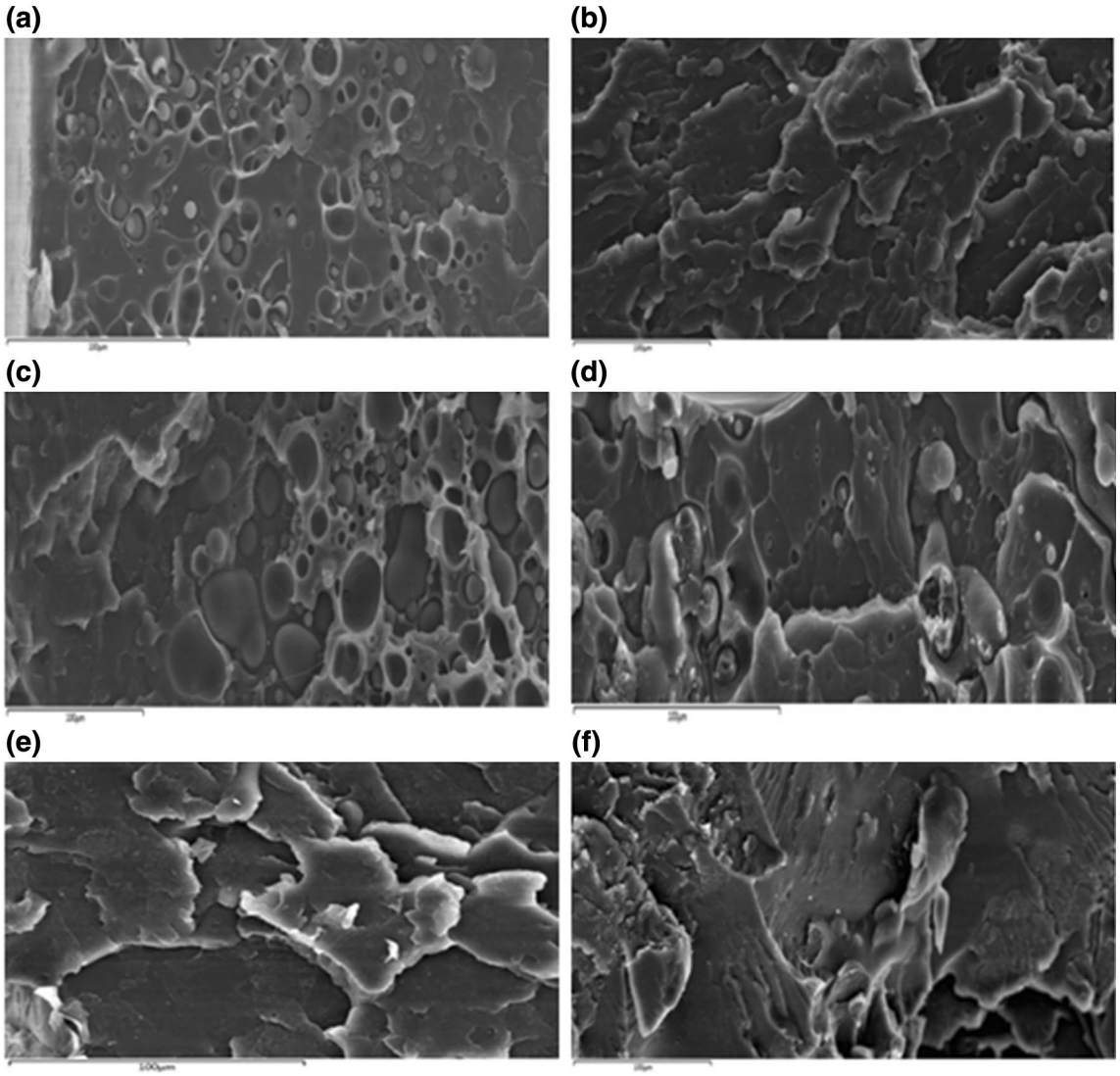

Fig. 11 Scanning electron micrographs of uncatalyzed and catalyzed PLA/PC blends: **a** (90/10), **b** (90/10/0.25%), **c** (70/30), **d** (70/30/0.25%), **e** (50/50), **f** (50/50/0.25%)

Conclusion

In this paper, thermal, viscoelastic and morphological properties of PLA/PC blends were investigated after being compounded without and with samarium acetylacetonate used as a transesterification catalyst between the two polymers.

The characterization of the uncatalyzed blends revealed their immiscibility for the studied compositions. DMTA results showed that the T_gs of the blends components are unchanged after blending without the catalyst. At temperatures below the PLA T_g, the uncatalyzed blends presented lower storage modulus which decreases further during the PLA glass transition, and then increases upon heating due to the cold crystallization process. A slight enhancement of the storage modulus is noticed for the (50/50) PLA/PC blend due the existence of a third phase that was also confirmed by the TG analysis. The study of the thermal properties by DSC showed the hindrance of the PLA crystallization due to the PC glassy phase which reduces the PLA chains mobility and causes the shift of the crystallization process towards higher temperatures, particularly when the PC content increases.

When the Sm-Acac catalyst was incorporated, immiscibility was still observed but several changes occurred on the blends properties. In one hand, the Sm-Acac acted as an efficient plasticizer by decreasing notably the T_gs of PC and PLA and affecting the crystallization behavior. In the other hand, it contributed to the promotion of a significant strengthening effect evidenced from the increase of the blends storage modulus in the temperature interval ranging between the end and the start of the PLA glass transition and cold crystallization events, respectively. The observation of such reinforcement suggested the contribution of chemical links to the enhancement of adhesion between the two phases in presence of the catalyst. After increasing the Sm-Acac catalyst concentration to 0.5%, a significant decrease in the polymers T_gs and the blends storage modulus is noticed as a result of the important Sm-Acac plasticization which prevented the strengthening effect that occurred for 0.25% of Sm-Acac. Also, a small peak attributable to the presence of the copolymer phase was noticed on the variations of Tan δ for the (90/10/0.5) PLA/PC/Sm-Acac blend. As a result of active interchange reactions, an amorphous copolymer having an intermediate T_g and a higher storage modulus was achieved from the (50/50/0.5) PLA/PC/Sm-Acac blend. Accordingly, the thermogravimetric analysis revealed a supplementary decomposition stage owing to the copolymer phase which presents its proper degradation characteristics. Also, it seems that the (50/50/0.25) PLA/PC/Sm-Acac blend offers an attractive combination that could provide a material presenting interesting properties until 90 °C due to the strengthening effect ensured by the copolymer synthesized via interchange reactions at the interface between PLA and PC.

References

1. Molinaro S, Cruz Romer M, Boaro M, Sensidoni A, Lagazio C, Morris M, Kerry J (2013) J Food Eng 117:113
2. Lai SM, Wu SH, Lin GG, Don TM (2014) Eur Polym J 52:193
3. Okamoto K, Toshima K, Matsumura S (2005) Macromol Biosci 5:813
4. Chang JH, An YU, G. Sur (2003) J Polym Sci 41:94
5. Ray SS, Okamoto M (2003) J Polym Sci 28:1539
6. Frone AN, Berlioz S, Chailan JF, Panaitescus DM (2013) Carbohydr Polym 91:377
7. Armentano I, Bitinis N, Fortunati E, Mattioli S, Rescignano N, Verdejo R, Lopez-Manchado MA, Kenny JM (2013) Prog Polym Sci 38:1720
8. Fortunati E, Luzi F, Puglia D, Dominici F, Santulli C, Kenny JM, Torre L (2014) Eur Polym J 56:77
9. Fortunati E, Armentano I, Zhou Q, Puglia D, Terenzi A, Berglund LA, Kenny JM (2012) Polym Degrad Stab 97:2027
10. Nan Wang Y, Xuan Weng Y, Wang L (2014) Polym Test 36:119
11. Araújo A, Botelho G, Oliveira M, Machado AV (2014) Appl Clay Sci 88–89:144
12. Rasal RM, Janorkar AV, Hirt DE (2010) Prog Polym Sci 35:338
13. Torres-Huerta AM, Palma-Ramírez D, Domínguez-Crespo MA, Del Angel-López D, de la Fuente D (2014) Eur Polym J 61:285
14. H. Chen, M. Pyda, P. Cebe (2009) Thermochim Acta 492:61.
15. Khankrua R, Piva-Art S, Hiroyuki H, Suttiruengwong S (2014) Polym Degrad Stab 108:232
16. G Biresaw, CJ Carriere (2004) Compos Part A 35:313.
17. Brito GF, Agrawal P, Araújo EM, de Mélo TJA (2012) Polímeros 22:427.
18. Jiang L, Wolcott MP, Zhang JW (2006) Biomacromolecules 7:199
19. Meaurio E, Zuza E, Sarasua JR (2005) Macromolecules 38:9221
20. Ayana B, Suin S, Khatua BB (2014) Carbohydr Polym 110:430
21. Malwela T, Ray SS (2012) Polymer 53:2705
22. T. J.A. Mélo, Araújo EM, Brito GF, Agrawal P (2013) J Alloys Compd 615:389
23. Hashima K, Nishitsuji S, Inoue T (2010) Polymer 51:3934
24. H. Zhao, Z. Cui, X. Wang, L.S. Turng, X. Peng (2013) Compos Part B 51:79.
25. Yang SL, Wu ZH, Yang W, Yang MB (2008) Polym Test 27:957
26. Jiang L, Zhang J, Wolcott MP (2007) Polymer 48:7632
27. Fukishima K, Tabuani D, Areana M, Gennari M, Camino G (2013) React Funct Polym 73:540
28. Hong N, Song L, Hu W, Hu Y (2013) Procedia Eng 62:366
29. Badrinarayanan P, Ko FK, Wang C, Richard BA, Kessler MR (2014) Polym Test 35:1
30. Cele HM, Ojijo V, Chen H, Kumar S, K. Land T, Joubert T, de Villiers MFR, Ray SS (2014) Polym Test 36:24
31. Żenkiewicz M, Richert J, Różański A (2010) Appl Clay Sci 29:251
32. Picard E, Espuche E, Fulchiron R (2011) Appl Clay Sci 53:58
33. R. Liu, S. Luo, J. Cao, Y. Peng (2013) Compos Part A 51:33.
34. Rahman MA, Santis DD, Spagnoli G, Ramorino G, Penco M, Phuong VT, Lazzeri A (2012) J Appl Polym Sci 10:38705
35. Gordobil O, Egués I, Llano-Ponte R, Labidi J (2014) Polym Degrad Stab 108:1
36. Shi Q, Zhoub C, Yueb Y, Guoa W, Wuc Y, Wub Q (2012) Carbohydr Polym 90:301

37. Abdulkhani A, Hosseinzideh J, Ashori A, Dadashi S, Takzare Z (2014) Polym Test 35:73
38. Koutsomitopoulou AF, Bénézet JC, Bergeret A, Papanicolaou GC (2014) Powder Technol 255:10
39. Pantani R, Gorrasi G, Vigliotta G, Murariu M, Dubois P (2013) Eur Polym J 49:3471
40. Nakayama N, Hayashi T (2007) Polym Degrad Stab 92:1255
41. Lee JB, Lee YK, Choi GD, Na SW, Park TS, Kim WN (2011) Polym Degrad Stab 96:553
42. Phuong VT, Coltelli MB, Cinelli P, Cifelli M, Verstichel S, Lazzeri A (2014) Polymer 55:4498
43. Liu C, Lin S, Zhou C, Yu W (2013) Polymer 53:313
44. Guessoum M, Haddaoui N (2006) Intern J Polym Mater 55:715.
45. Guessoum M, Fenouillot-Rimilinger F, Haddaoui N (2008) Intern J Polym Mater 57:657.
46. Guessoum M, Nekkaa S, Haddaoui N (2008) Intern J Polym Mater 57:759.
47. Ignatov VN, Carraro C, Tartari V, Pippa R, Scapin M, Pilati F, Berti C, Toselli M, Fiorini M (1997) Polymer 38:195
48. Ignatov VN, Carraro C, Tartari V, Pippa R, Scapin M, Pilati F, Berti C, Toselli M, Fiorini M (1997) Polymer 38:201
49. Berti C, Bonora V, Pilati F, Fiorini M (2002) Makromol Chem 193:1665.
50. Fiorini M, Berti C, Ignatov VN, Toselli M, Pilati F (1995) J Appl Polym 55:1157
51. Fiorini M, Pilati F, Berti C, Toselli M, Ignatov VN (1997) Polymer 38:413
52. Ignatov VN, Carraro C, Tartari V, Pippa R, Pilati F, Berti C, Toselli M, Fiorini M (1996) Polymer 37:5883
53. Marchese P, Celli A, Fiorini M (2002) Macromol Chem Phys 203:695
54. Zhang JM, Tashiro K, Tsuji H, Domb JA (2008) Macromolecules 41:1352
55. Zhang J, Duan Y, Sato H, Tsuji H, Noda I, Yan S, Ozaki Y (2005) Macromolecules 38:8012
56. Djellali S, Sadoun T, Haddaoui N (2015) Polym Bull 72:1177.
57. Pluta M (2014) Polymer 45:8239
58. Pluta M, Murariu M, Alexandre M, Galeski A, Dubois P (2008) Polym Degrad Stab 93:925
59. Silverajah VS, Ibrahim AN, Yunus WZW, Hassan HA, Woei CB (2012) Intern J Molecul Sci 13:5878.
60. Chen HM, Chen J, Yang LN, Huang T, Zhang N, Wang Y (2013) J Polym Sci Part B 51:183.
61. Martınez-Hernandez AL, Velasco-Santos C, de-Icaza M, Castano VM (2007) Compos Part B 38:405.
62. Keusch S, Haessler R (1999) Compos Part A 30:997.
63. Shieh YT, Lin YS, Twu YK, Tsai HB, Lin RH (2010) J Appl Polym Sci 116:1334
64. Ismail HM (1995) Colloids Surf A 97:247.